

# The myocardial phenotype of Fabry disease pre-hypertrophy and pre-detectable storage

João B. Augusto <sup>1,2†</sup>, Nicolas Johner <sup>3†</sup>, Dipen Shah<sup>3</sup>, Sabrina Nordin <sup>1,2</sup>,  
 Kristopher D. Knott <sup>1,2</sup>, Stefania Rosmini<sup>2</sup>, Clement Lau <sup>2,4</sup>, Mashaef Alfarid <sup>1,2</sup>,  
 Rebecca Hughes <sup>1,2</sup>, Andreas Seraphim<sup>1,2</sup>, Ravi Vijapurapu <sup>5</sup>, Anish Bhuvu<sup>1,2</sup>,  
 Linda Lin <sup>2</sup>, Natalia Ojrzynska<sup>2,6</sup>, Tarekegn Geberhiwot<sup>7</sup>, Gabriella Captur <sup>2</sup>,  
 Uma Ramaswami<sup>8</sup>, Richard P. Steeds <sup>5</sup>, Rebecca Kozor<sup>9</sup>, Derralynn Hughes<sup>8</sup>,  
 James C. Moon <sup>1,2</sup>, and Mehdi Namdar<sup>3\*</sup>

<sup>1</sup>Institute of Cardiovascular Science, University College London, London, UK; <sup>2</sup>Department of Cardiovascular Imaging, Barts Heart Centre, Barts Health NHS Trust, London, UK; <sup>3</sup>Cardiology Division, Geneva University Hospitals, Rue Gabrielle-Perret-Gentil 4, 1205 Geneva, Switzerland; <sup>4</sup>William Harvey Research Institute, NIHR Barts Biomedical Research Centre, Queen Mary University of London, London, UK; <sup>5</sup>Cardiology Department, University Hospitals Birmingham, Birmingham, UK; <sup>6</sup>Institute of Cardiology, Warsaw, Poland; <sup>7</sup>Inherited Metabolic Disorders Unit, University Hospitals Birmingham, Birmingham, UK; <sup>8</sup>Royal Free London NHS Foundation Trust and University College London, London, UK; and <sup>9</sup>Sydney Medical School, University of Sydney, Sydney, Australia

Received 16 March 2020; editorial decision 11 April 2020; accepted 15 April 2020

## Aims

Cardiac involvement in Fabry disease (FD) occurs prior to left ventricular hypertrophy (LVH) and is characterized by low myocardial native T1 with sphingolipid storage reflected by cardiovascular magnetic resonance (CMR) and electrocardiogram (ECG) changes. We hypothesize that a pre-storage myocardial phenotype might occur even earlier, prior to T1 lowering.

## Methods and results

FD patients and age-, sex-, and heart rate-matched healthy controls underwent same-day ECG with advanced analysis and multiparametric CMR [cines, global longitudinal strain (GLS), T1 and T2 mapping, stress perfusion (myocardial blood flow, MBF), and late gadolinium enhancement (LGE)]. One hundred and fourteen Fabry patients (46 ± 13 years, 61% female) and 76 controls (49 ± 15 years, 50% female) were included. In pre-LVH FD ( $n = 72$ , 63%), a low T1 ( $n = 32/72$ , 44%) was associated with a constellation of ECG and functional abnormalities compared to normal T1 FD patients and controls. However, pre-LVH FD with normal T1 ( $n = 40/72$ , 56%) also had abnormalities compared to controls: reduced GLS ( $-18 \pm 2$  vs.  $-20 \pm 2\%$ ,  $P < 0.001$ ), microvascular changes (lower MBF  $2.5 \pm 0.7$  vs.  $3.0 \pm 0.8$  mL/g/min,  $P = 0.028$ ), subtle T2 elevation ( $50 \pm 4$  vs.  $48 \pm 2$  ms,  $P = 0.027$ ), and limited LGE (%LGE  $0.3 \pm 1.1$  vs.  $0\%$ ,  $P = 0.004$ ). ECG abnormalities included shorter P-wave duration ( $88 \pm 12$  vs.  $94 \pm 15$  ms,  $P = 0.010$ ) and T-wave peak time ( $T_{\text{onset}} - T_{\text{peak}}$ ;  $104 \pm 28$  vs.  $115 \pm 20$  ms,  $P = 0.015$ ), resulting in a more symmetric T wave with lower T-wave time ratio ( $(T_{\text{onset}} - T_{\text{peak}})/(T_{\text{peak}} - T_{\text{end}})$ ) ( $1.5 \pm 0.4$  vs.  $1.8 \pm 0.4$ ,  $P < 0.001$ ) compared to controls.

## Conclusion

FD has a measurable myocardial phenotype pre-LVH and pre-detectable myocyte storage with microvascular dysfunction, subtly impaired GLS and altered atrial depolarization and ventricular repolarization intervals.

## Keywords

Fabry disease • cardiovascular magnetic resonance • electrocardiogram • microvascular dysfunction • global longitudinal strain

\* Corresponding author. Tel: +41 22 372 71 92; Fax: +41 22 372 72 29. E-mail: mehdi.namdar@hcuge.ch

† The first two authors contributed equally to this work.

© The Author(s) 2020. Published by Oxford University Press on behalf of the European Society of Cardiology.

This is an Open Access article distributed under the terms of the Creative Commons Attribution Non-Commercial License (<http://creativecommons.org/licenses/by-nc/4.0/>), which permits non-commercial re-use, distribution, and reproduction in any medium, provided the original work is properly cited. For commercial re-use, please contact [journals.permissions@oup.com](mailto:journals.permissions@oup.com)

## Introduction

Fabry disease (OMIM 301500; FD) is a rare X-linked lysosomal storage disorder caused by mutations in the  $\alpha$ -galactosidase A gene (*GLA*). The consequence is progressive sphingolipid accumulation<sup>1</sup> affecting multiple organs. Since the availability of renal replacement therapy, the main cause of death has been cardiac, through heart failure or arrhythmia.<sup>2,3</sup> Therapy is available for FD (enzyme replacement and oral chaperone therapies) but the effect is incomplete likely due to late initiation. The presence of overt left ventricular hypertrophy (LVH) and myocardial fibrosis has been shown to negatively affect treatment outcome, suggesting the importance of early initiation of treatment.<sup>4</sup> Whilst treating all from diagnosis is not an option due to the therapeutic and financial burden,<sup>5</sup> the optimal timing of intervention is not known. Cardiac response to treatment is typically assessed by measuring the left ventricular (LV) mass, but this method does not quantify myocardial biology or earlier stages when the benefit could be exploited. Better description of myocardial disease stages and processes might lead to a better understanding of the earliest commitment to irreversible disease and opportunity to commence treatment.<sup>4</sup>

Cardiovascular magnetic resonance (CMR) is a key tool for studying cardiac manifestations of FD. Early descriptions were of LVH and late gadolinium enhancement (LGE) in the basal inferolateral wall, thought initially to reflect only fibrosis.<sup>6–8</sup> Later, multiparametric CMR has been able to measure sphingolipid infiltration (T1 mapping, low native T1)<sup>9</sup> and apparent oedema (T2 mapping, high native T2) with blood troponin elevation suggesting inflammation.<sup>10,11</sup> A pre-LVH phase of cardiac FD was subsequently defined by a low T1 phenotype, occurring in up to 60% of FD patients; slightly elevated LV ejection fraction and electrocardiographic (ECG) changes were also observed pre-LVH.<sup>12,13</sup>

However, as sphingolipid storage starts before birth<sup>14</sup> and T1 mapping presumably has a detection threshold, a 'silent' sphingolipid accumulation stage before T1 lowers must also occur. To explore this, new techniques would be needed. By CMR, two pathways and their measurement techniques show promise. First, global longitudinal strain (GLS), which is robustly measured and changes earlier in many diseases including FD.<sup>15</sup> Second, myocardial blood flow (MBF) measured by stress perfusion mapping, which reflects smooth muscle/endothelial changes that occur early in FD.<sup>16</sup>

A third approach has also been suggested. The 'traditional' 12-lead ECG is informative in FD, with some of the first reports of abnormal ECG in FD being published in the 1970s.<sup>17</sup> Since then, several ECG features have been described in FD: atrioventricular (AV) block, short and long PQ interval, changes in QRS width and repolarization abnormalities, associated with arrhythmias and disease progression.<sup>18–20</sup> Some features, particularly with advanced ECG analysis, occur early, pre-LVH and include accelerated atrial and ventricular depolarization/conductivity (shortening of P-wave duration and QRS width),<sup>21</sup> with sphingolipid storage as a potential cause.<sup>19</sup>

Accordingly, we hypothesized that an even earlier phase of cardiac FD (pre-LVH, pre-low-T1) might be identifiable using a combination of CMR perfusion mapping, GLS assessment, and advanced 12-lead surface ECG analysis.

## Methods

### Study population

Fabry patients were recruited from the Lysosomal Storage Disorders Unit at Royal Free Hospital (RFH) London between 2015 and 2019, as part of the prospective Fabry400 study (NCT03199001). We included all consecutive FD patients with a confirmed *GLA* mutation (Supplementary data online, Table S1), multiparametric CMR and same day ECG. Patients <18 years old, with standard contraindications to CMR or with known pregnancy were excluded.

In addition, we included age-, sex-, and heart rate-matched healthy controls who also underwent parametric CMR and same day ECG. The healthy control group were volunteers free of any history or symptoms of cardiovascular disease or other comorbidities, and who were not taking any medications.

The study conformed to the principles of the Helsinki Declaration and ethical approval was obtained for both study groups. Written informed consent was obtained from all participants.

### Clinical data and blood biomarkers

Clinical data collected included enzyme replacement and oral chaperone therapies status, *GLA* variant (Supplementary data online, Table S1), body surface area (BSA), and systolic and diastolic peripheral blood pressures. All FD patients had blood collected just before the scan and analysed for high-sensitivity troponin T (hsTnT, normal <15 ng/L) and NT-proBNP (brain natriuretic peptide, normal <47 pmol/L).

### ECG analysis

Twelve-lead surface ECG was acquired at rest (Welch Allyn CP 200 Electrocardiograph) and independently analysed by two experts in a consensus reading (N.J. and M.N.), blinded to both clinical status (patient or healthy control) and CMR. Measurements were taken manually from the tracings at a sweep of 25 mm/s and standard criteria and normal values for ECG findings were applied (Supplementary data online, Methods).

### P wave and PQ interval

P-wave indices were recorded in lead II. Atrial dimensions are known to affect the P-wave morphology and duration, and thus the PQ interval, which is why a 'corrected' PQ interval was derived by measuring the PQ interval minus P-wave duration in lead II ( $P_{\text{end}} - Q$ ), better reflecting AV conduction.<sup>22</sup>

### QRS complex

QRS axis (degrees) and the presence of left bundle branch block or right bundle branch block (RBBB), incomplete RBBB or intraventricular conduction delay (100–120 ms) were recorded. ECG LVH criteria were assessed using Sokolow–Lyon index [S-wave voltage in V1 + R-wave voltage in V5 or V6 (whichever larger) >35 mm], Cornell index [(R-wave voltage in aVL + S-wave voltage in V3)  $\times$  QRS duration  $\geq$ 2440 mm·ms for males (adding 8 mm for females)], and the ratio between T- and R-wave amplitudes in V5 (T-wave amplitude measured in the concordant part with R wave). R-wave amplitude in V1 was also recorded (a prominent R in V1 can be a marker of septal LVH or right ventricular hypertrophy). Presence of fractionated QRS (fQRS, a marker of intraventricular conduction delay) was checked for each patient and the number of leads with fQRS was noted.

### T wave

The time interval between the onset and the peak of T wave ( $T_{\text{onset}} - T_{\text{peak}}$ ) and from the peak until the end of the T wave ( $T_{\text{peak}} - T_{\text{end}}$ ), an index

of transmural dispersion of ventricular repolarization<sup>23</sup>) were recorded in II or V5; in the presence of negative or biphasic T wave, the peak was measured from the nadir of the T wave and leads with T waves with less than 1.5 mm in amplitude were excluded from the analysis. A measure of T-wave skewness/symmetry was calculated as the ratio between  $T_{\text{onset}} - T_{\text{peak}}$  and  $T_{\text{peak}} - T_{\text{end}}$ . Pathological repolarization was defined as a discordant ST/T as compared to the main QRS axis.

We also noted the presence of atrial fibrillation and atrial and/or ventricular pacing. None of the patients had higher than first degree AV block. ECG intervals of interest are summarized in Figure 1.

## CMR acquisition

All participants underwent CMR at 1.5 Tesla (Avanto or Aera, Siemens Healthcare, Erlangen, Germany) in one of three centres: the Heart Hospital, Barts Heart Centre, or Chenies Mews Imaging Centre. Standard cine imaging for ventricular volume analysis was performed.<sup>3</sup> Native T1 mapping was performed on four-chamber, three-chamber views, and three (basal, mid, and apical) LV short-axis (SAX) slices using a modified Look-Locker inversion recovery sequence (MOLLI, 5b[3s]3b). Native T2 mapping was acquired on the same slices using a steady-state free-precession sequence in 99 Fabry patients and 26 controls. Adenosine stress perfusion mapping was performed in 45 Fabry patients (32 were LVH negative) and 27 controls<sup>16</sup> (most common reason for not being performed was patient preference). Stress perfusion images were obtained in the basal, mid, and apical LV SAX slices. LGE images were acquired (not performed in eight patients due to contrast contraindication)

following a bolus of 0.1 mmol/kg gadolinium contrast agent (Gadoterate meglumine, Dotarem, Guerbet S.A., France) using a phase sensitive inversion recovery sequence. Post-contrast T1 mapping was performed 15 min after gadolinium administration on the same location as native T1 for extracellular volume fraction (ECV) quantification. The T1 Mapping and ECV Standardization Program (T1MES) phantom was scanned to quality control for T1 and T2 mapping stability across all sites; the results have been published elsewhere.<sup>3,12,16</sup>

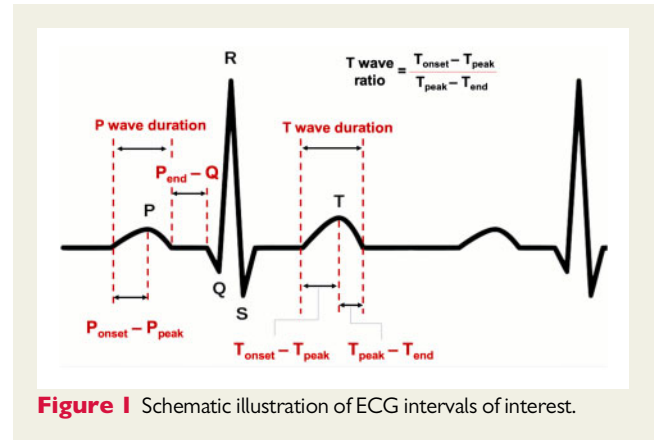


**Figure 1** Schematic illustration of ECG intervals of interest.

**Table 1** Clinical and cardiovascular magnetic resonance findings in healthy controls and Fabry patients without LVH

	Healthy controls (n = 76)	Fabry disease without LVH		P-value normal T1 vs. healthy controls	P-value normal T1 vs. low T1
		Normal T1 (n = 40)	Low T1 (n = 32)		
Age (years)	49 ± 15	40 ± 13	43 ± 11	<b>0.002</b>	0.332
Male, n (%)	38 (50)	5 (13)	8 (25)	<b>&lt;0.001</b>	0.222
SBP (mmHg)	122 ± 13	110 ± 11	115 ± 11	<b>&lt;0.001</b>	0.155
DBP (mmHg)	76 ± 9	71 ± 8	75 ± 5	<b>0.010</b>	0.082
BSA (m <sup>2</sup> )	1.8 ± 0.2	1.8 ± 0.2	1.8 ± 0.2	0.448	0.753
Cardiac variant, n (%)	NA	13 (33)	10 (31)		1.000
ERT/OCT, n (%)	NA	13 (33)	12 (38)		0.804
hs-TnT (ng/L)	NA	1 (1–5)	3 (1–6)		0.693
NT-proBNP (pmol/L)	NA	8 (1–14)	6 (1–12)		0.630
CMR					
LV EDVI (mL/m <sup>2</sup> )	72 ± 11	74 ± 11	72 ± 12	0.437	0.564
LVEF (%)	67 ± 4	70 ± 7	73 ± 6	<b>0.018</b>	0.097
LVMI (g/m <sup>2</sup> )	65 ± 13	59 ± 10	67 ± 14	<b>0.008</b>	<b>0.011</b>
MWT (mm)	9 (7–10)	8 (7–9)	10 (9–11)	0.527	<b>0.001</b>
Septal T1 (ms)	1029 ± 38	1000 ± 28	913 ± 35	<b>&lt;0.001</b>	<b>&lt;0.001</b>
BIFL T2 (ms)	48 ± 2	50 ± 4	46 ± 2	<b>0.027</b>	<b>0.021</b>
Global ECV	24 ± 3	26 ± 2	25 ± 2	<b>0.029</b>	0.243
LGE, n (%)	0	5/37 (14)	8/31 (26)	<b>0.003</b>	0.230
LV LGE (%) <sup>a</sup>	0	0.3 ± 1.1	0.7 ± 1.4	<b>0.004</b>	0.156
GLS (%)	-20.3 ± 2.3	-18.3 ± 2.1	-18.7 ± 2.5	<b>&lt;0.001</b>	0.457
Stress MBF (mL/g per min)	3.0 ± 0.8	2.5 ± 0.7	2.5 ± 0.5	<b>0.028</b>	0.961

BIFL, basal inferolateral wall; BNP, brain natriuretic peptide; BSA, body surface area; CMR, cardiovascular magnetic resonance; DBP, diastolic blood pressure; ECV, extracellular volume fraction; EDVI, end-diastolic volume index; ERT, enzyme replacement therapy; GLS, global longitudinal strain; hs-TnT, high-sensitivity troponin T; LGE, late gadolinium enhancement; LVEF, left ventricular ejection fraction; LVH, left ventricular hypertrophy; LVMI, left ventricular mass index; MBF, myocardial blood flow; MWT, maximum wall thickness; NA, not available/not applicable; OCT, oral chaperone therapy; SBP, systolic blood pressure.

<sup>a</sup>Non-normally distributed variable.





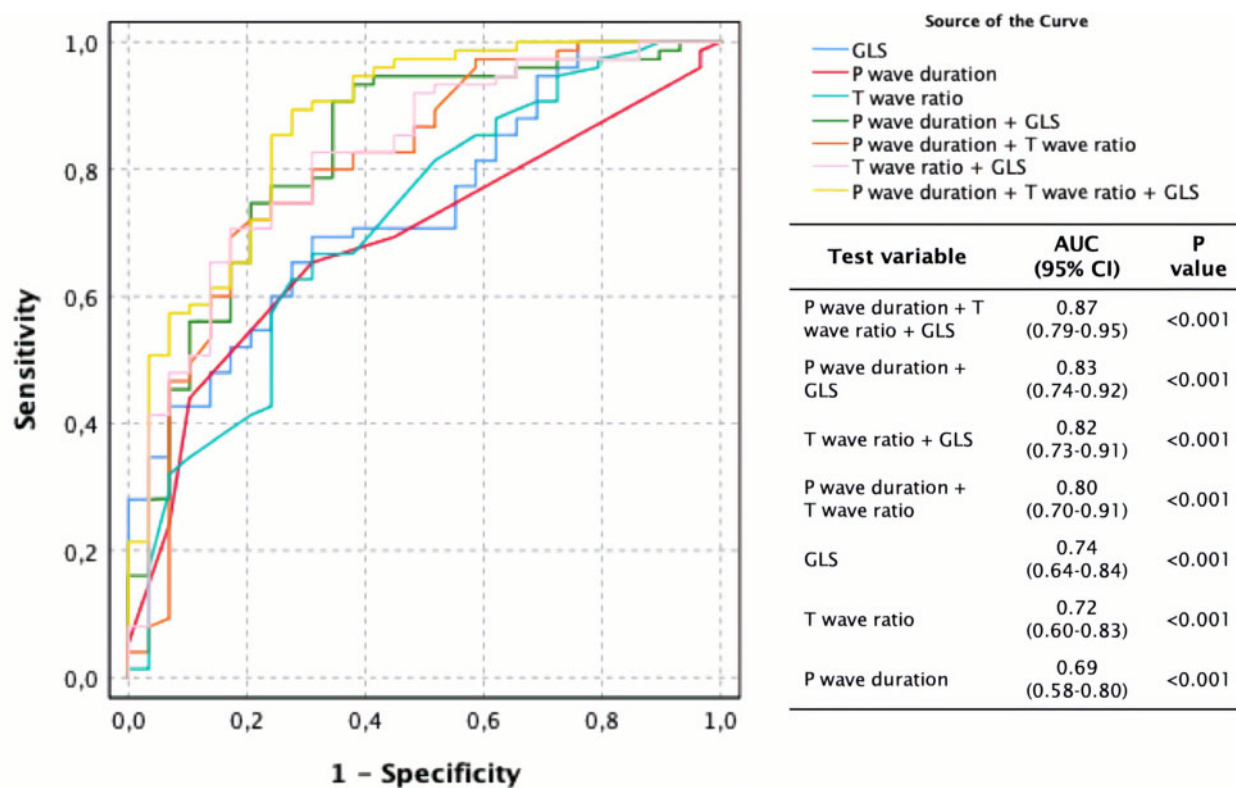
**Table 3** Uni- and multivariable regression analysis of the determinants of very early cardiac involvement in Fabry disease (pre-LVH and normal T1 mapping)

Dependent variable	Variables in model	P-value	Multivariable Exp(B) (95% CI)	P-value
Normal T1, No LVH FD (vs. controls)	GLS, per 1% decrease	<0.001	2.9 (1.2–7.2)	<b>0.026</b>
	Global stress MBF, per 1 mL/g/min decrease	<b>0.035</b>	2.1 (0.4–9.7)	0.353
	%LV LGE, per 1% increase	0.996		
	BIFL T2, per 1 ms increase	<b>0.038</b>	1.0 (0.6–1.7)	0.985
	ECV, per 1% increase	<b>0.037</b>	0.5 (0.2–1.4)	0.181
	PQ interval, per 1 ms decrease	<b>0.020<sup>a</sup></b>		
	P-wave duration, per 1 ms decrease	<b>0.020</b>	1.2 (1.0–1.5)	<b>0.029</b>
	$T_{\text{onset}} - T_{\text{peak}}$ , per 1 point decrease	<b>0.021<sup>b</sup></b>		
	$T_{\text{peak}} - T_{\text{end}}$ , per 1 point increase	0.058		
	$(T_{\text{onset}} - T_{\text{peak}})/(T_{\text{peak}} - T_{\text{end}})$ , per 1 point decrease	<b>0.001</b>	976 (2.2–425219)	<b>0.026</b>
T-wave amplitude, per 1 mm decrease	<b>0.001</b>	1.4 (0.7–2.6)	0.363	

BIFL, basal inferolateral; CI, confidence interval; ECV, extracellular volume fraction; FD, Fabry disease; GLS, global longitudinal strain; LGE, late gadolinium enhancement; LV, left ventricular; LVH, LV hypertrophy; MBF, myocardial blood flow.

<sup>a</sup>P-wave duration was included instead.

<sup>b</sup>T-wave time ratio was included instead.

**Figure 3** Receiver-operator characteristic curves and corresponding AUCs for detection of cardiac involvement in pre-hypertrophic normal T1 Fabry disease. AUC, area under the curve; CI, confidence interval; GLS, global longitudinal strain.

mm·ms,  $P=0.006$ ] (Tables 1 and 2). GLS was lower ( $-18.3 \pm 2.1$  vs.  $-20.3 \pm 2.3\%$ ,  $P<0.001$ ) as was stress MBF ( $2.5 \pm 0.7$  vs.  $3.0 \pm 0.8$  mL/g/min,  $P=0.028$ ). There was slightly higher BIFL T2 ( $50 \pm 4$  vs.  $48 \pm 2$  ms,  $P=0.027$ ), ECV ( $26 \pm 2$  vs.  $24 \pm 3\%$ ,  $P=0.029$ ), and %LGE

( $0.3 \pm 1.1$  vs.  $0\%$ ,  $P=0.004$ ) than controls. PQ was shorter ( $152 \pm 27$  vs.  $163 \pm 22$ ms,  $P=0.017$ ), mostly due to shorter P-wave duration ( $88 \pm 12$  vs.  $94 \pm 15$  ms,  $P=0.010$ ) with lower T-wave amplitudes [ $3$  ( $2-4$ ) vs.  $4$  ( $3-6$ ) mm,  $P<0.001$ ] and shorter  $T_{\text{onset}} - T_{\text{peak}}$  ( $104 \pm 28$

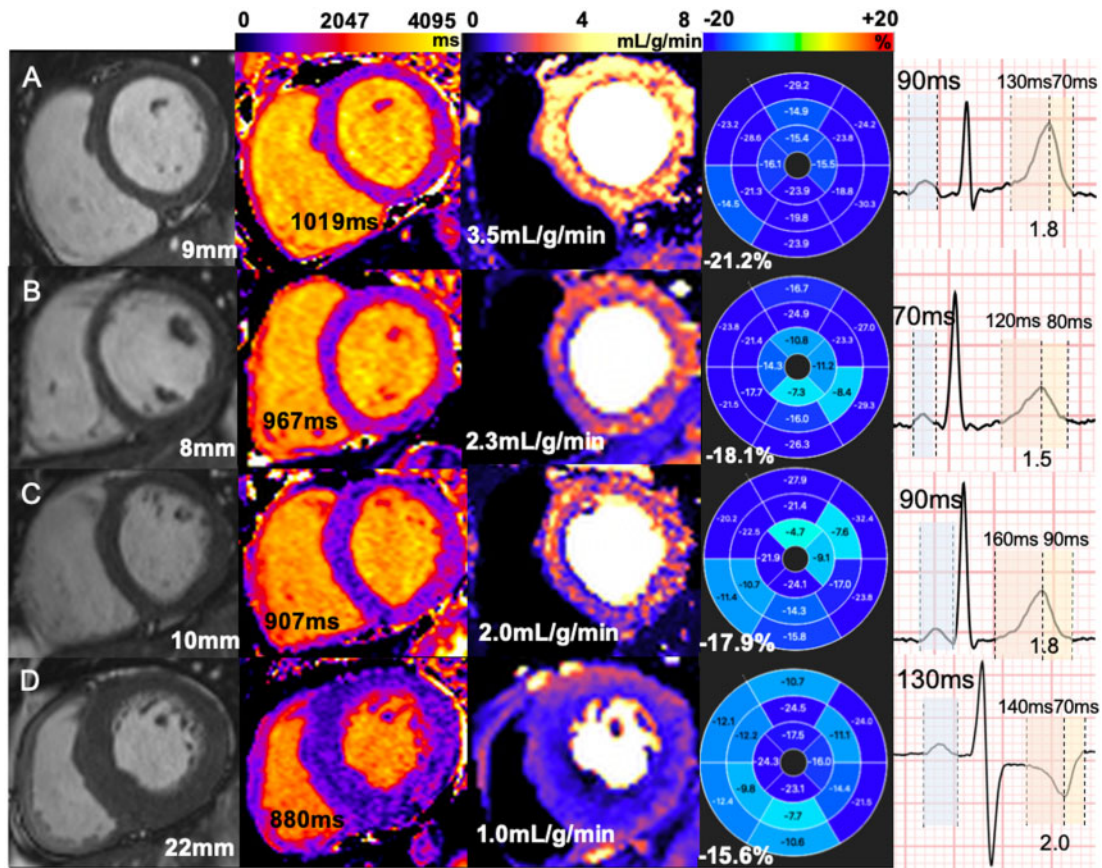


**Figure 4** Multiparametric cardiovascular magnetic resonance and electrocardiographic assessment in patients with FD and healthy controls. Left to right—steady-state free precession cines, native T1 mapping, stress MBF mapping, GLS, P-wave duration, and T-wave ratio. (A) Healthy control, no LVH, normal T1, MBF, GLS, P-wave time, and T-wave ratio. (B) FD with normal T1 and without LVH; MBF and GLS are mildly reduced, P wave is short and T-wave ratio reduced. (C) FD with low T1 and without LVH, low MBF and GLS, P-wave duration, and T-wave ratio are no different from control. (D) FD with LVH; T1 is low, MBF and GLS are significantly impaired, P wave is long and T-wave ratio increased.

vs.  $115 \pm 20$  ms,  $P=0.015$ ) but longer  $T_{\text{peak}} - T_{\text{end}}$  ( $72 \pm 14$  vs.  $67 \pm 12$  ms,  $P=0.053$ ), resulting in significantly lower  $(T_{\text{onset}} - T_{\text{peak}})/(T_{\text{peak}} - T_{\text{end}})$  ratio ( $1.5 \pm 0.4$  vs.  $1.8 \pm 0.4$ ,  $P<0.001$ ) than controls (Table 2 and Supplementary data online, Table S5).

### Very early FD: observation robustness

To assess the robustness of these changes, biomarkers of interest (GLS, MBF, T2, ECV, %LV LGE, PQ interval, P-wave duration,  $T_{\text{onset}} - T_{\text{peak}}$ ,  $T_{\text{peak}} - T_{\text{end}}$ ,  $[T_{\text{onset}} - T_{\text{peak}}]/[T_{\text{peak}} - T_{\text{end}}]$  and T-wave amplitude) were selected for regression analysis (Table 3). GLS [2.9, 95% confidence interval (1.2–7.2),  $P=0.026$ ], P-wave duration [1.2 (1.0–1.5),  $P=0.029$ ] and  $(T_{\text{onset}} - T_{\text{peak}})/(T_{\text{peak}} - T_{\text{end}})$  ratio [976 (2.2–425219),  $P=0.026$ ] predict very early cardiac FD involvement (pre-LVH normal T1) in multivariable regression analysis. The three aforementioned variables were computed in ROC curve analysis, either isolated or in combination (Figure 3, Supplementary data online, Results). The best discriminative ability however was a ROC curve that used the logit value of all three variables combined (see Supplementary data online, Results)—area under the curve (AUC) 0.87 (0.79–0.95,  $P<0.001$ ), significantly superior to other curves'

AUC ( $P<0.05$  for all). A selection of findings across subgroups is summarized in Figure 4.

## Discussion

In recent years, a pre-hypertrophic phase of FD with ECG abnormalities and sphingolipid storage detected by T1 mapping has been described. Here, we sought an even earlier phase of cardiac FD pre-LVH and pre-detectable storage by using advanced ECG analysis and two CMR methods, GLS measurement and quantitative perfusion mapping. In both overt and pre-LVH disease with storage, we found the expected changes in all parameters. For pre-LVH, pre-detectable storage there was an identifiable phenotype with lower ECG conventional voltages than healthy volunteers, and a number of other more robust features: reduced MBF and GLS, PQ shortening (mainly from a shorter P-wave duration), and a shorter  $T_{\text{onset}} - T_{\text{peak}}$  time (with a shorter  $(T_{\text{onset}} - T_{\text{peak}})/(T_{\text{peak}} - T_{\text{end}})$  ratio also). Prior staging of Fabry cardiomyopathy<sup>3</sup> included a pre-LVH stage (accumulation/storage) and two LVH stages (hypertrophy and inflammation; fibrosis and

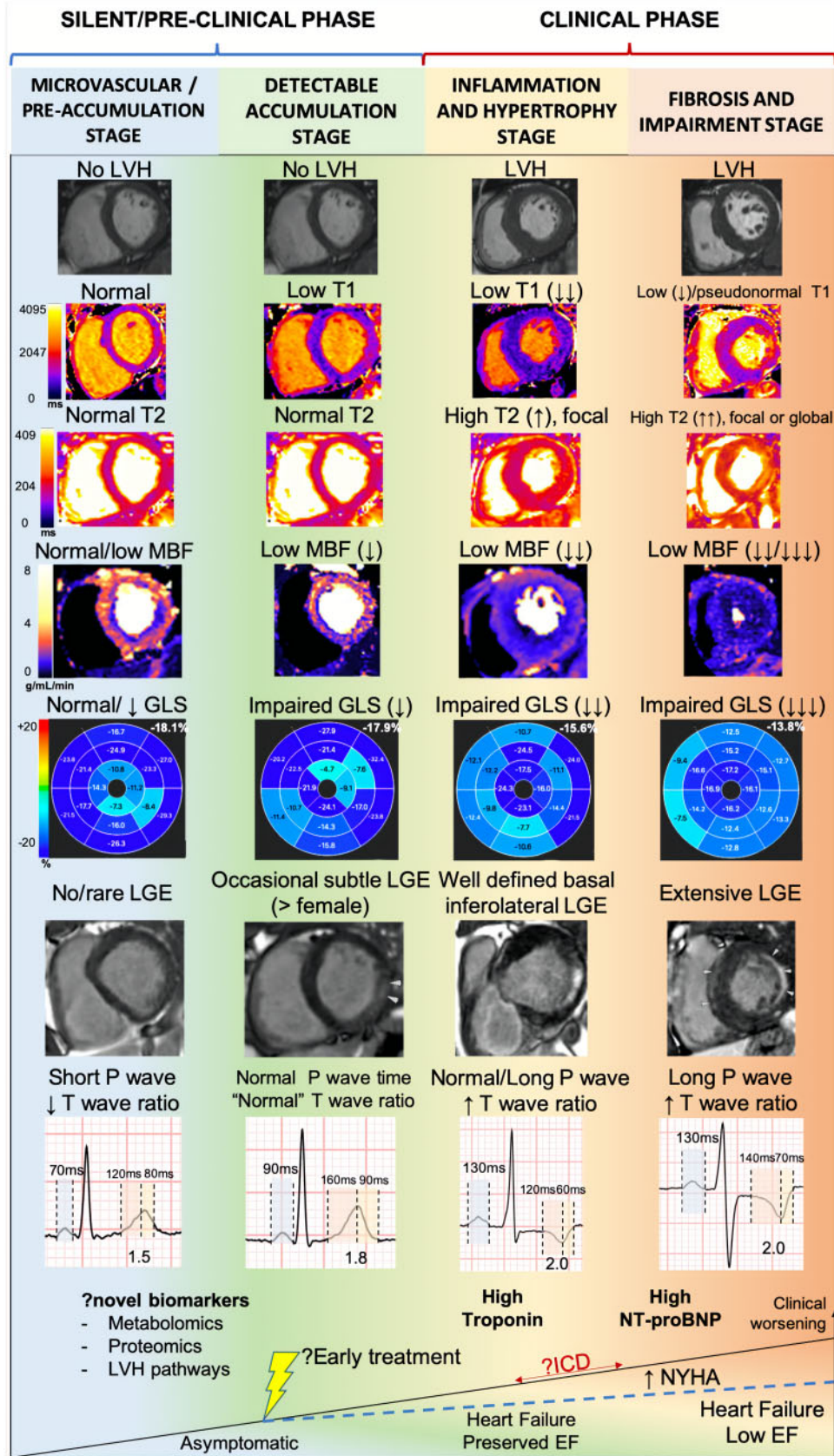


**Figure 5** Proposed stages of cardiac involvement in Fabry disease. A new pre-storage stage is proposed.



2. Baig S, Edward NC, Kotecha D, Liu B, Nordin S, Kozor R et al. Ventricular arrhythmia and sudden cardiac death in Fabry disease: a systematic review of risk factors in clinical practice. *Europace* 2017;**20**:f153–61.
3. Nordin S, Kozor R, Medina-Menacho K, Abdel-Gadir A, Baig S, Sado DM et al. Proposed stages of myocardial phenotype development in Fabry disease. *JACC Cardiovasc Imaging* 2018;**12**:1673–83.
4. Weidemann F, Niemann M, Breunig F, Herrmann S, Beer M, Störk S et al. Long-term effects of enzyme replacement therapy on Fabry cardiomyopathy: evidence for a better outcome with early treatment. *Circulation* 2009;**119**:524–9.
5. Eng CM, Guffon N, Wilcox WR, Germain DP, Lee P, Waldek S et al. Safety and efficacy of recombinant human alpha-galactosidase A replacement therapy in Fabry's disease. *N Engl J Med* 2001;**345**:9–16.
6. Moon JC, Sheppard M, Reed E, Lee P, Elliott PM, Pennell DJ. The histological basis of late gadolinium enhancement cardiovascular magnetic resonance in a patient with Anderson-Fabry disease. *J Cardiovasc Magn Reson* 2006;**8**:479–82.
7. Moon JCC, Sachdev B, Elkington AG, McKenna WJ, Mehta A, Pennell DJ et al. Gadolinium enhanced cardiovascular magnetic resonance in Anderson-Fabry disease. Evidence for a disease specific abnormality of the myocardial interstitium. *Eur Heart J* 2003;**24**:2151–5.
8. Krämer J, Niemann M, Störk S, Frantz S, Beer M, Ertl G et al. Relation of burden of myocardial fibrosis to malignant ventricular arrhythmias and outcomes in Fabry disease. *Am J Cardiol* 2014;**114**:895–900.
9. Sado DM, White SK, Piechnik SK, Banyersad SM, Treibel T, Captur G et al. Identification and assessment of Anderson-Fabry disease by cardiovascular magnetic resonance noncontrast myocardial T1 mapping. *Circ Cardiovasc Imaging* 2013;**6**:392–8.
10. Nordin S, Kozor R, Bulluck H, Castelletti S, Rosmini S, Abdel-Gadir A et al. Cardiac Fabry disease with late gadolinium enhancement is a chronic inflammatory cardiomyopathy. *J Am Coll Cardiol* 2016;**68**:1707–8.
11. Augusto JB, Nordin S, Vijapurapu R, Baig S, Bulluck H, Castelletti S et al. Myocardial edema, myocyte injury, and disease severity in Fabry disease. *Circ Cardiovasc Imaging* 2020;**13**:e010171.
12. Nordin S, Kozor R, Baig S, Abdel-Gadir A, Medina-Menacho K, Rosmini S et al. Cardiac phenotype of prehypertrophic Fabry disease. *Circ Cardiovasc Imaging* 2018;**11**:e007168.
13. Camporeale A, Pieroni M, Pieruzzi F, Lusardi P, Pica S, Spada M et al. Predictors of clinical evolution in prehypertrophic Fabry disease. *Circ Cardiovasc Imaging* 2019;**12**:e008424.
14. Vedder AC, Strijland A, Vd Bergh Weerman MA, Florquin S, Aerts J, Hollak C. Manifestations of Fabry disease in placental tissue. *J Inherit Metab Dis* 2006;**29**:106–11.
15. Vijapurapu R, Nordin S, Baig S, Liu B, Rosmini S, Augusto J et al. Global longitudinal strain, myocardial storage and hypertrophy in Fabry disease. *Heart* 2019;**105**:470–6.
16. Knott KD, Augusto JB, Nordin S, Kozor R, Camaioni C, Xue H et al. Quantitative myocardial perfusion in Fabry disease. *Circ Cardiovasc Imaging* 2019;**12**:e008872.
17. Roudebush CP, Foerster JM, Bing OH. The abbreviated PR interval of Fabry's disease. *N Engl J Med* 1973;**289**:357–8.
18. Namdar M, Kampmann C, Steffel J, Walder D, Holzmeister J, Lüscher TF et al. PQ interval in patients with Fabry disease. *Am J Cardiol* 2010;**105**:753–6.
19. Namdar M. Electrocardiographic changes and arrhythmia in Fabry disease. *Front Cardiovasc Med* 2016;**3**:7.
20. Schmied C, Nowak A, Gruner C, Olinger E, Debaix H, Brauchlin A et al. The value of ECG parameters as markers of treatment response in Fabry cardiomyopathy. *Heart* 2016;**102**:1309–14.
21. Niemann M, Hartmann T, Namdar M, Breunig F, Beer M, Machann W et al. Cross-sectional baseline analysis of electrocardiography in a large cohort of patients with untreated Fabry disease. *J Inherit Metab Dis* 2013;**36**:873–9.
22. Namdar M, Steffel J, Jetzer S, Schmied C, Hürlimann D, Camici GG et al. Value of electrocardiogram in the differentiation of hypertensive heart disease, hypertrophic cardiomyopathy, aortic stenosis, amyloidosis, and Fabry disease. *Am J Cardiol* 2012;**109**:587–93.
23. Tse G, Gong M, Wong WT, Georgopoulos S, Letsas KP, Vassiliou VS et al. The T<sub>peak</sub>–T<sub>end</sub> interval as an electrocardiographic risk marker of arrhythmic and mortality outcomes: a systematic review and meta-analysis. *Heart Rhythm* 2017;**14**:1131–7.
24. Maceira AM, Prasad SK, Khan M, Pennell DJ. Normalized left ventricular systolic and diastolic function by steady state free precession cardiovascular magnetic resonance. *J Cardiovasc Magn Reson* 2006;**8**:417–26.
25. Antzelevitch C. Cellular basis and mechanism underlying normal and abnormal myocardial repolarization and arrhythmogenesis. *Ann Med* 2004;**36**:5–14.